Physics Letters A 378 (2014) 95–99

Contents lists available at ScienceDirect

Physics Letters A

www.elsevier.com/locate/pla

Electron dynamics triggered by double attosecond pulses: Simulations based on time-dependent density functional theory

Yalong Jiao [a], Feng Wang [b,*], Xuhai Hong [a], Wenyong Su [a], Zhen Zhang [c]

[a] School of Physics, Key Laboratory of Cluster Science of Ministry of Education, Beijing Institute of Technology, Beijing 100081, China
[b] Laser Micro/Nano Fabrication Laboratory, School of Mechanical Engineering, Beijing Institute of Technology, Beijing 100081, China
[c] School of Software, Beijing Institute of Technology, Beijing 100081, China

ARTICLE INFO

Article history:
Received 2 September 2013
Received in revised form 16 October 2013
Accepted 31 October 2013
Available online 6 November 2013
Communicated by R. Wu

Keywords:
Time-dependent density functional theory
Electron dynamics
Attosecond pulse
Polarization angle

ABSTRACT

In order to observe the high-field effect, the external laser field must reach its peak intensity before the electron ionization. To this end, it is important to reduce pulse duration to typical attosecond timescale. In this paper, the interaction electron dynamics between attosecond pulses and dielectric is investigated within the time-dependent density functional theory. Taking the CaF_2 crystal as an example, we give a comparison of electron dynamics response between single and double pulses. Moreover, the nonlinear energy absorption and electron excitation processes are simulated by adjusting the polarization direction of the sub-pulse. Present results demonstrate that the double pulses show lower electron excitation and energy absorption than the single pulse, which is in accordance with experimental higher ablation threshold and smaller heat-affected zones of the double pulses. In addition, the curves of final excited electron number and energy absorption exhibit the quasi-symmetry about the axis of 180°, which has not been reported yet.

1. Introduction

The rapid development in the field of the laser technology enables increasing pulse power and reducing pulse duration, and a wide range of previously unreachable areas dominated by nonlinear electron excitations become accessible. The attosecond pulse, produced by the high-order harmonic generation, is of great importance for the progress of the ultrafast science. Unlike general nanosecond, picosecond, femtosecond pulse, the attosecond pulse allows the use of much higher effective field intensity within the ultrashort time scale before the electrons have time to be ionized [1]. Furthermore, the attosecond pulse explores areas of deeply investigating fundamental physical processes on electronic or atomic timescales such as observation and control of electron dynamics in atoms [2–4], molecules [5] and solids [6].

Laser–material interaction is a fundamental process with abundant nonlinear dynamics. It is a good approximation to state that the ultrafast laser is absorbed by electrons due to the much smaller mass of electrons than the nucleus, which denotes the investigation of electron excitation process is of importance during the interaction process. Several different electron excitation mechanisms are proposed below: for weak electric field ionization of an electron requires that the incoming photon energy must exceed the binding energy of the electron, however, as field strength increases, the nonlinear effects dominate and strong-field ionization (or excitation) mechanisms such as multiple photons and tunnel ionization [7] become important. In order to excite an electron, it is necessary to supply enough energy to bridge the gap from its initial state (the valence band) to an available final state (the conduction band). Once excited to the conduction band, the “free” electrons may be accelerated again by the laser field and enable further excitation of the bound electrons possibly by collisional excitation mechanism.

Due to the limitation of experimental technique, the researches down to attosecond scale cannot be widely carried out, which impels one to resort to the theoretical simulations for predicting the electron dynamics effect under the ultrafast intense laser pulses. In order to obtain the desired electron dynamics process, it is essential to implement the relevant controls by adjusting the pulse parameters such as peak intensity [8], pulse number [9], wavelength [10], interpulse delay [11], etc. Especially, the modulation of sub-pulse polarization can greatly increase the degree of attainable control, which has not been reported in detail both in theory and experiment. Therefore it is important in our work to study laser–material interaction process by adjusting the sub-pulse polarization direction in attosecond scale. A reliable prediction is expected to promote the development of such experiments.

The main structure of the paper is as follows. In Section 2, we introduce the theoretical framework briefly and calculations in

* Corresponding author. Tel.: +86 10 68914732.
E-mail address: wangfeng01@tsinghua.org.cn (F. Wang).

0375-9601/$ – see front matter
http://dx.doi.org/10.1016/j.physleta.2013.10.053

detail. In Section 3, the electron dynamics in CaF_2 under the laser consisting of single pulse and double pulses are compared, then, the excited electron number and total energy absorption are given as the function of polarization angles. A conclusion is given in Section 4. Atomic units (abbreviated a.u.) are used throughout this paper unless otherwise specified.

2. Theory

The time-dependent density functional theory (TDDFT) has been used as an effective tool for the control of electron dynamics [12,13] with a reasonable accuracy at moderate computational cost. A brief description of TDDFT is summarized below.

For N-electron quantum system, a set of Kohn–Sham orbitals (KSO) $\psi_n(\vec{r},t)$ satisfy the time-dependent Kohn–Sham equations with the following form:

$$i\hbar\frac{\partial}{\partial t}\psi_n(\vec{r},t) = H_{ks}(\vec{r},t)\psi_n(\vec{r},t), \tag{1}$$

where H_{ks} is the Kohn–Sham Hamiltonian, which can be expressed as

$$H_{ks}(\vec{r},t) = \frac{1}{2m}\left(\vec{P}+\frac{e}{c}\vec{A}(t)\right)^2 + V_{ion}(\vec{r},t) + \int d^3\vec{r}'\frac{\rho(\vec{r}',t)}{|\vec{r}-\vec{r}'|} + V_{xc}(\vec{r},t), \tag{2}$$

where $V_{ion}(\vec{r},t)$ is the electron–ion potential, $V_{xc}(\vec{r},t)$ is the exchange correlation (xc) potential, $\rho(\vec{r},t)$ is the time-dependent density given by $\sum_n^{occ}|\psi_n(\vec{r},t)|^2$. In the first item, $\vec{A}(t)$ is the total spatially uniform vector potential, which is composed of the external and induced vector potentials, $\vec{A}(t) = \vec{A}_{ex}(t) + \vec{A}_{in}(t)$. $\vec{A}_{ex}(t)$ is converted to the laser field $\vec{E}_{laser}(t)$ by the relation of $\vec{E}_{laser}(t) = -d\vec{A}_{ex}(t)/dt$. The induced vector potential $\vec{A}_{in}(t)$ is caused by the charge accumulation at the surface induced by the polarization of the external field [14].

The laser field is defined with the following form:

$$E_{laser}(t) = E_0\sin(\omega t)\sin^2\left(\frac{\pi t}{T}\right) \tag{3}$$

where ω is the laser frequency, T is the duration time, E_0 is the maximum amplitude of the electric field. In practical calculations, the total electric field is proportional to the applied field approximately by $E \approx \varepsilon^{-1}E_{laser}$, where ε is the static dielectric constant of the material [15].

The number of excited electrons $n_{ext}(t)$ per unit cell is defined as [12]

$$n_{ext}(t) = \sum_{nn'}\delta_{nn'} - \sum_{nn'k}\left(\left|\langle\phi_{nk}|\psi_{n'k}(t)\rangle\right|^2\right) \tag{4}$$

where n and n' represent the orbital index and k is the Bloch wave number. The first term gives the total electron number, and the second term is the unexcited electron number which is expressed as the modulus square of the orbital wavefunction at time t projecting to the ground state. In present simulation, the $\{|\phi_{nk}\rangle\}$ is a basic set including 32 occupied orbitals, which is obtained through ground state calculation.

At the end of laser, the excited electron distribution in the conduction band is defined by the modulus square of the projection of the final orbitals to the initial particle states,

$$n_{occ}(m,k) = \sum_{m'}\left(\left|\langle\varphi_{mk}|\psi_{m'k}(T)\rangle\right|^2\right) \tag{5}$$

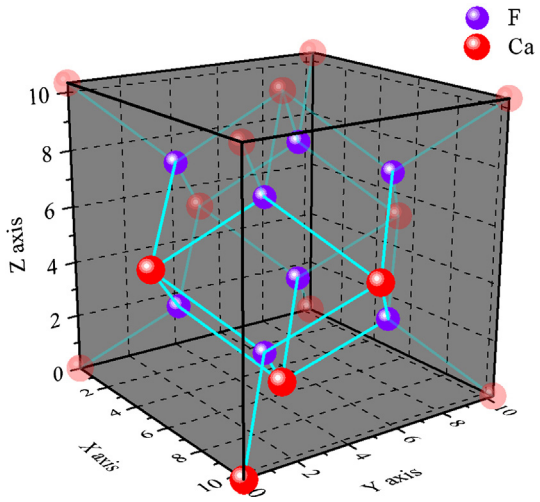

Fig. 1. The geometrical diagram of CaF_2 crystal in a unit cell. The calcium and fluorine atoms are represented by the red and violet balls, respectively. The semitransparent red balls are also calcium atoms but not included in the practical calculation. (For interpretation of the references to color in this figure legend, the reader is referred to the web version of this article.)

where T is the total propagation time, m and m' represent the particle states. The basic set $\{|\varphi_{mk}\rangle\}$ includes 32 occupied and 40 unoccupied orbitals in practical calculation.

The calculations within the framework of TDDFT are implemented in real-time, real-space and first-principles code Octopus [16]. The interaction between valance electrons and ion cores is described by the norm-conserving Troullier–Martins pseudopotentials [17]. A high-order finite difference formula is used for the Laplacian operator. The local-density approximation (LDA) [18] with the Perdew–Zunger parametrization [19] is employed as the xc functional [20]. The enforced time-reversal symmetry (ETRS) [21] is used to propagate the KSO. It is noted that the ion cores are set to be static during the time evolution of laser because the typical attosecond pulse is so short to stimulate the ion dynamics.

3. Calculation results and discussion

Fig. 1 shows the geometrical diagram of CaF_2 crystal in a unit cell, which is a promising laser material with a wide band gap of 12.1 eV [22]. Its lattice constant is 10.324 a.u. [23]. The unit cell includes 8 fluorine atoms (violet balls) and 4 calcium atoms (red balls). In our calculations, the KSO are represented on the $25\times25\times25$ spatial grid points with each mesh spacing of 0.413 a.u. to ensure a convergent calculation. The propagation time per laser pulse T_{pulse} is 33 a.u. (798 as) with each time step of 0.025 a.u. to ensure a stable time evolution. The number of k-points is $12\times12\times12$ in reciprocal space cell. In consideration of symmetries, the irreducible 84 k-points are used practically in the Brillouin zone. The laser parameters are set as: the maximum amplitude E_0 of 0.883 a.u., the frequency of 0.518 a.u. from the experiment [24].

Fig. 2 shows the comparison of energy absorption and excited electron under the single pulse and double pulses. They have the equal peak intensities and duration time. At the beginning of the pulses, there is no obvious energy absorption, because the transition selection rule still works due to the low intensity, and the electrons cannot be effectively excited through coupling with photons. For the single pulse (a1), as the increase of the electric field from 0.2 fs, nonlinear effects dominate and the absorbed energy curve starts to rise with oscillation which derives from the stimulated emission. After 1.2 fs, although the absorbed energy reaches the saturation value, the curve of the excited electron still